Role of suspension preparation in the spray drying process to obtain nano/submicrostructured YSZ powders for atmospheric plasma spraying

Pablo Carpio[1,*], Rodrigo Moreno[2], Andrés Gómez[3], María Dolores Salvador[4], Enrique Sánchez[1]

(1) Instituto de Tecnología Cerámica (ITC), Universitat Jaume I (UJI). Castellón, Spain

(2) Instituto de Cerámica y Vidrio (ICV), CSIC. Madrid, Spain

(3) Institut de Ciència dels Materials (ICM), Parc Cientific, Universitat de València (UV). Valencia, Spain

(4) Instituto de Tecnología de Materiales (ITM), Universitat Politècnica de València (UPV). Valencia, Spain

Pablo Carpio ([*]corresponding author)

Email: pablo.carpio@itc.uji.es   Telephone number: (+34) 964 342424

Postal address: Instituto de Tecnología Cerámica (ITC). Campus Universitario Riu Sec.

Av. Vicent Sos Baynat s/n

12006 Castellón (Spain)

Rodrigo Moreno

Email: rmoreno@icv.csic.es

Andrés Gómez:

Email: andres.gomez@uv.es

María Dolores Salvador

Email: dsalva@mcm.upv.es

Enrique Sánchez

Email: enrique.sanchez@itc.uji.es

Abstract

Thermal barrier coatings were manufactured by atmospheric plasma spray process from YSZ powders. These powders were made by a reconstitution process which consists in a spray-drying of suspensions followed by thermal treatment of the granules.

Nano- and submicron-sized YSZ particles were used as starting material. Feeding well dispersed suspension to spray-drying chamber is the first key step in the reconstitution process. With this aim, concentrated, stable YSZ suspensions were obtained by means of the optimisation of the preparation conditions. Then reconstituted granules were produced by spray-drying of the YSZ suspensions and the following thermal treatment which was optimised.

The reconstituted powders were then successfully deposited on austenitic stainless steel coupons by APS. The findings in this work proved that the reconstituted powders characteristics which in turn are related to the starting suspension properties affect the final coating microstructure in terms of the amount of unmelted zones.

1. Introduction

Yttria stabilised zirconia (YSZ) ceramics are used in a variety of structural and functional applications due to their good mechanical properties over a wide temperature range [1,2]. In particular, YSZ layers are used as top coat of thermal barrier coatings (TBCs) because of their superior high-temperature properties, such as low thermal conductivity, high toughness and relatively high thermal expansion coefficient [3]

One of the most implemented techniques to manufacture TBCs is atmospheric plasma spraying (APS) [4]. It consists in the injection within a high-energy plasma flow of a feed material where this later encounters melting and accelerating until it impacts upon substrate. On the substrate, molten (or partially molten) material is quickly cooled forming individual lamellae, the stacking of which forming the coating [5].
Conventional YSZ powders for thermal barrier coatings are obtained by different methods such as fusion and crushing, spray-drying, sol-gel, milling and sintering or spheodisation. The typical coating microstructure obtained from these powders is laminar formed by flattened drops or *splats* with some microstructural features as voids or cracks which affect the coating properties. The characteristics of the feeding powders strongly affect these microstructural features [5].
By spraying nanoparticles instead of conventional micrometric powders, coatings can be obtained that exhibit different architectures and enhanced properties [6,7]. However, nanoparticles cannot be directly sprayed because of their low mass and poor flowability. To overcome these problems, three possible routes can be found in the literature: to reconstitute the individual nanoparticles into spherical micrometre-sized granules; to inject directly a suspension of nanoparticles (Suspension Plasma Spraying or SPS); or to inject a solution precursor of the coating (Solution Precursor Plasma Spraying or SPPS) [5,8]. The first route was followed in this work and spray drying from a nanoparticle suspension is one of the most widely used agglomeration method. Often spray-drying is followed by thermal treatment of the resulting nanostructured granules to enhance their sinterability [9-11]. Thermal spray deposition of such agglomerates leads to a two-scale

microstructure that basically comprises unmelted agglomerates (nanozones) surrounded by fully melted areas, which act as binder matrix [4]. Such a coating structure is typified most of the time as bimodal structure.

Feeding of a well dispersed suspension to spray-drying chamber is of paramount importance if homogeneous spray-dried granules with high apparent specific weight are to be obtained [12]. Colloidal processing needs to be interpreted to control the interparticle force during all processing stages. Besides when nanoparticles are used suspension stabilisation becomes critical as a consequence of the extremely high interparticle interactions associated with fine particles [13]. Nevertheless most of papers about YSZ coatings obtained from nanostructured, powders go through the feedstock preparation process without giving any details about colloidal processing of the nanoparticle suspension to be spray-dried.

Nanozirconia colloidal processing has been largely studied in the recent literature. Some works have reported the effect of different types of dispersants [14,15] or the effect of solid loadings [16-18]. In fact, some authors have obtained YSZ granules by spray-drying and freeze-drying but the starting suspensions were quite diluted and the granules obtained were then highly porous (apparent specific mass of 230-1200 kg/m^3) [19-21]. One way of overcoming this problem is by using mixtures of nano/submicron-sized particles. Adding coarser particles to a nanozirconia suspension can reduce considerably the suspension viscosity due to particle packing enhancement making the suspension preparation and handling easy and allowing the achievement of higher solid loadings in the final suspension [22]. A recent study on alumina-titania APS coatings obtained from nano/submicron-sized particles mixtures reported an improvement of mechanical properties of the coatings when compared with coatings deposited from exclusively nanostructured powders. According to that work when the binary mixture was used denser and more homogeneous spray-dry agglomerates were obtained which improved the microstructure of the final coatings [23].

The first part of this work addresses the preparation of concentrated, stable YSZ suspensions from nano- and submicron-sized particles by assessing the suspension preparation conditions: dispersant content, sonication time, solids loading and particle size distribution (nano/submicronsized ratio). Then reconstituted granules were produced by spray-drying of the YSZ suspensions and subsequent thermal treatments. Finally these granules were deposited by APS. The work firstly aims at relating the suspension preparation step with agglomerates characteristics and secondly the effect of feedstock agglomerates on microstructure features of the final coating.

2. Experimental

2.1. Materials

A commercial YSZ nanoparticle powder (5932HT, Nanostructured and Amorphous Materials Inc., USA), and a commercial YSZ submicron-sized powder (TZ-3YS, Tosoh Co., Japan) were used as raw materials. The main characteristics as provided by the suppliers are shown in table 1.

Furthermore, a commercial salt (DURAMAX^{TM} D-3005, Rohm & Haas/Dow Chemicals, USA) of polyacrylic acid-based polyelectrolyte (PAA), with 35 wt% active matter was used in order to performance the colloidal stability of the powders in water. The amount of dispersant in the prepared suspensions was referred in wt.% in relation to

the YSZ content.This dispersant has been used in other previous works with nanozirconia powders [16].

The nanoparticles were characterised by transmission electronic microscopy (TEM, H7100, Hitachi, Japan), specific surface area was determined using the single-point BET method (Monosorb, Quantachrome Co., USA) and crystalline phases were identified by X-ray diffraction (XRD D8 Advance, Bruker AXS, Germany).

Particle size distribution of submicron-sized particles was determined with a laser diffraction analyzer (Matersizer S, Malvern, UK) while dynamic light scattering (DLS) analyzer (Zetasizer NanoZS, Malvern, UK) was used in the case of nanoparticles. In this last case adding different dispersant content in nanoparticle suspension with very low solid loading (0.01 wt% YSZ) and a sonication probe (UP 400S, Dr Hielscher GmbH, Germany) was used in order to avoid agglomerations which can interfere in the analysis. Suspensions were cooled in an ice-water bath during sonication to avoid excessive heating.

2.2. Suspension preparation and characterisation

The colloidal stability of YSZ powders was studied by zeta potential measurements as a function of dispersant content and pH. The equipment employed was the same as that used for the particle size distribution. In order to perform the measurements, diluted suspensions with 0.01 wt% YSZ and KCl 0.01M as electrolyte were prepared. The pH values were determined with a pH-meter (Titrino DMS 716, Metrohm, Switzerland) and were adjusted with HCl and KOH solutions.

Nanoparticle suspensions were prepared by adding YSZ nanopowder to the dispersing medium (optimal quantity of dispersant into water) using a blade-stirrer. In order to breakdown any agglomerate present, the suspensions were dispersed with a sonication probe. Rheological behaviour at different dispersant contents, sonication time and solid loading were studied.

In addition, suspension from submicron-sized particles with a solid content of 30 vol.% was also obtained. An optimal amount of dispersant was used and different sonication times were tested. Then bimodal suspensions with a solid content of 30 vol.% and different nano/submicron-sized particle ratios were prepared. For this purpose, nano- and submicron-sized particle suspension were prepared separately, using an optimal amount of dispersant (different for each suspension and previously calculated) and sonication time. After the single-component suspensions were mixed with a blade-stirrer during 30 min and the resultant suspensions were again performed under the sonication test.

The rheological behaviour of all suspensions was determined using a rotational rheometer (Mars, Thermo Haake Co., Thermo, Germany) operating at controlled shear rate (CR) by loading the shear rate from 0 to 1000 s^{-1} in 300 s, maintaining at 1000 s^{-1} for 60 s and uploading from 1000 to 0 s^{-1} in 300 s. The measurements were carried out at 25 ºC using a double-cone and plate system [24].

In order to study the ageing effect of the suspensions, the rheological behaviour was determined after 7 days from the suspension preparation time. During this time, suspensions were maintained under agitation with a low speed orbital shaker [25,26].

2.3. Powder reconstitution process

Spray-dried granules from different suspensions were obtained by spray-drying (Mobile Minor, Gea Niro, Denmark) with a drying capacity of 7 kg water/h [27]. Then the spray-dried powders were heat treated in an electric kiln at temperatures ranging from 850 °C to 1400 °C, with a 60-min soaking time. As reported elsewhere the thermal treatment aims to consolidate the feedstock particle to avoid any breakdown during feedstock delivery and to enhance the agglomerate sinterability for the following, extremely fast sintering process in the plasma torch [11]. The optimal thermal treatment temperature was considered when granule porosity was slightly reduced without allowing an excessive grain-growth inside the granule. Therefore, contraction curves by heating microscopy (Misura 3, Expert System Solutions, Italy) were carriet out to know the sinterability range of the granules. Then granules were treated at different temperatures which were chosen from contraction curves and microstructure inspection.

Untreated and thermally treated powders were characterised before the APS deposition. The crystalline phases were determined by XRD and a field-emission scanning electron microscope (S-4800, Hitachi, Japan) was used to analyse feedstock microstructure. Granule apparent specific mass ($\rho_{granule}$) was calculated from powder tapped specific mass by assuming a theoretical packing factor of 0.6, which is characteristic of monosized, spherical particles [28]. Powder flowability was evaluated in terms of the Hausner ratio, which is the ratio of the tapped specific mass to the apparent specific mass. Free-flowing powders display a Hauser ratio below 1.25 [28].

## 2.4. Coatings processing and characterisation

YSZ coatings were deposited by an atmospheric plasma spray (APS) system. It consisted of a gun (F4-MB, Sulzer Metco, Germany) operated by an industrial robot (IRB 1400, ABB, Switzerland). Before spraying, the substrate was grit blasted with brown corundum, with an average particle size of 250 µm and at the pressure was of $4.2 \cdot 10^5$ Pa. The grit blasted substrates were cleaned with ethanol to remove any remaining dust or grease from the surface. A bond coat (AMDRY 997, Sulzer-Metco, Germany) was used to enhance the adhesion between the substrate and the ceramic layer. The bond coat composition was Ni-23Co-20Cr-9Al-4.2Ta-0.6Y (wt%) according to supplier information. Deposition was performed using argon and hydrogen as plasma-forming gases. The main spraying parameters are listed in table 2.

In order to evaluate the differences between the coatings, coating microstructure was investigated by FEG-SEM. The micrographs were obtained on polished cross sections of the different coatings.

3. Results and discussion

3.1. Starting raw materials characterisation

The microstructural observation of the YSZ nanoparticles, made by TEM, shows that the particles were agglomerated with an average particle size of approximately 40 nm (figure 1). Figure 2 shows the particle size distribution of the nanopowder at different PAA content. As it can be seen at 2% PAA addition no further dispersion is obtained. The measured mean particle size of nanoparticles was 48 nm which agrees well with the data obtained from the TEM observation as well as with the value given by the supplier.
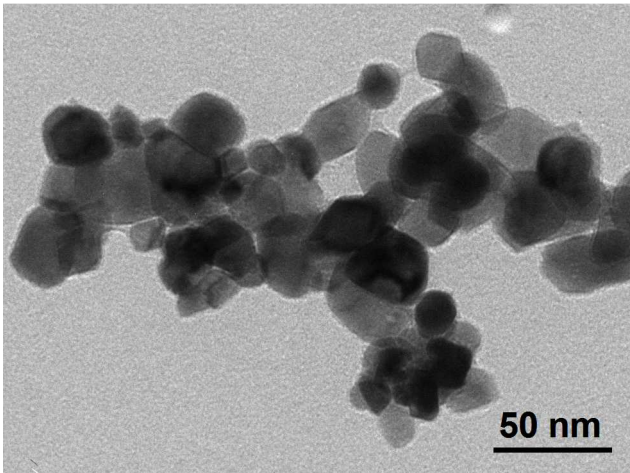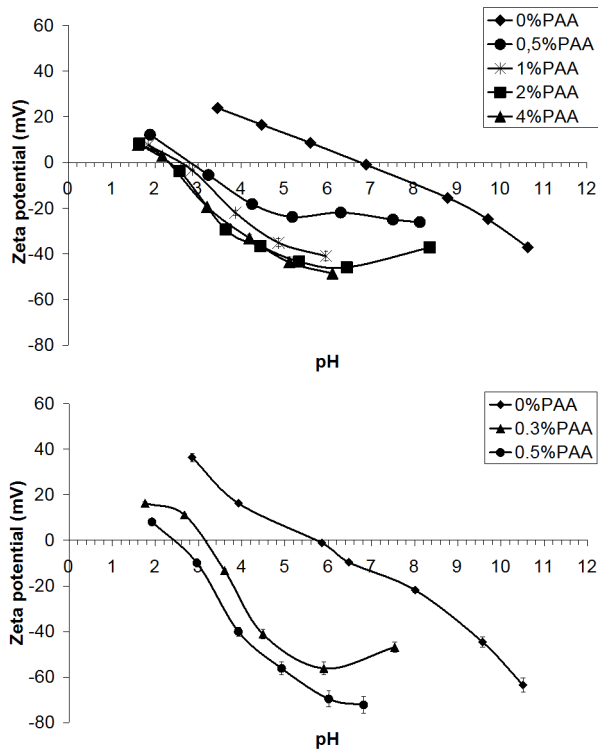
Figure 1
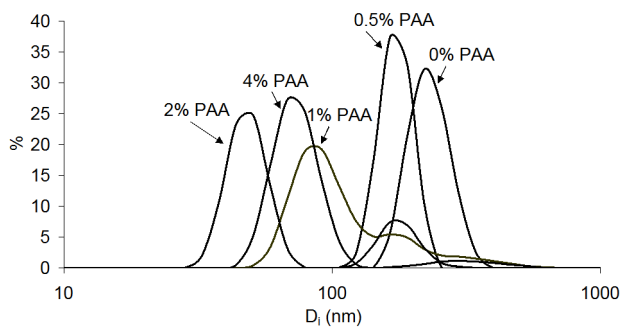
Figure 2

Specific surface areas of nano- and submicron-sized particle were 25.1 and 6.8 m^2g^{-1} respectively. Unlike supplier's data the diffractogram pattern of nanopowder revealed the tetragonal phase as the main crystalline phase together with monoclinic phase (30 mol%).

### 3.2. Suspension preparation and characterisation

Figure 3 shows the evolution of zeta potential of nano- and submicron-sized YSZ powders without dispersant and with different contents of PAA. The isoelectric point (IEP) of these powders without additives occurs at 6.2 and 6.9 respectively, in good agreement with the values reported in the literature [15-17]. In both cases, IEP shifted to acid pH as the PAA content increased. This demonstrates that PAA was adsorbed leading to well dispersed suspensions at working pH. Zeta potential curve does not change significantly for PAA contents >2 wt% in the case of nanoparticle suspension and >0.5 wt% in the case of submicron-sized suspension (not shown in the figure). It means that only these amounts of PAA were adsorbed on the particles. In addition, these results also agree with particle size measurements at different PAA contents. Consequently, the calculated amount of adsorbed dispersant in both cases was 0.8 mg/m^2. Similar amount of adsorbed dispersant were determined in other works that dispersed other powders using the same dispersant [11,12].

Figure 3

Once the colloidal characterisation with diluted suspension was funded, higher concentration suspensions were prepared so as to proceed to the rheological characterisation to analyse the influence of dispersant content, sonication time, solids loading and ageing on the rheological behaviour. In addition, the effect of nano/submicron-sized particle ratio on this rheology behaviour was also assessed.

Figure 4 shows the flow curves of 20 vol.% YSZ nanoparticle suspension at two different PAA content. As it can be seen viscosity and thixotropy (hysteresis loop in the flow curve) of 4% PAA suspension were lower than those of the 2% suspension. However it was concluded above that a maximum of 2 wt% of PAA was adsorbed on the nanoparticle surface. This apparent paradox could be explained by the fact that other dispersion mechanism rather than electrosteric repulsion could contribute to system stabilisation. Thus a combination between electrosteric and depletion dispersion in which some dispersant molecules are free in suspension seems to occur resulting in higher consumption of dispersant [29]. This fact also explains that more concentrated suspensions (higher than 20.vol%) with 2% PAA could not be prepared. Hence, from now on, YSZ nanoparticle suspensions were prepared using 4 wt% PAA.
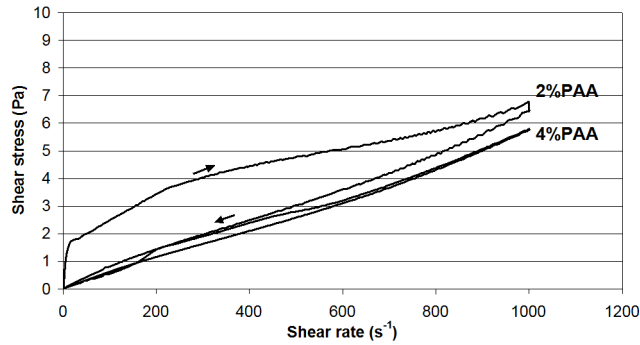
Figure 4

On the other hand a sonication test is always necessary to disperse nanoparticle in suspensions [24,29]. Sonication time is to be optimised for every system since too long sonication time gives rise to agglomeration. Figure 5 shows rheological behaviour of 10 vol.% (~39.6 wt%), 20 vol.% (~59.6 wt%), 30 vol.% (~71.6 wt%) and 35 vol.% (~76.1 wt%) nanoparticle suspensions just as prepared and after exposure to different sonication times. As expected, it can be observed that sonicated suspensions show lower viscosity whereas this effect was more pronounced at higher solid loadings. The thixotropic cycle in the 10 vol. % nanoparticle suspensions did not appear but it occurred at higher concentration. Hence sonication leaded to remove thixotropic cycle in the case of 20 vol.% while in 30 vol.% and 35 vol.% it was considerably reduced. In all cases, optimal sonication time was 3 minutes.
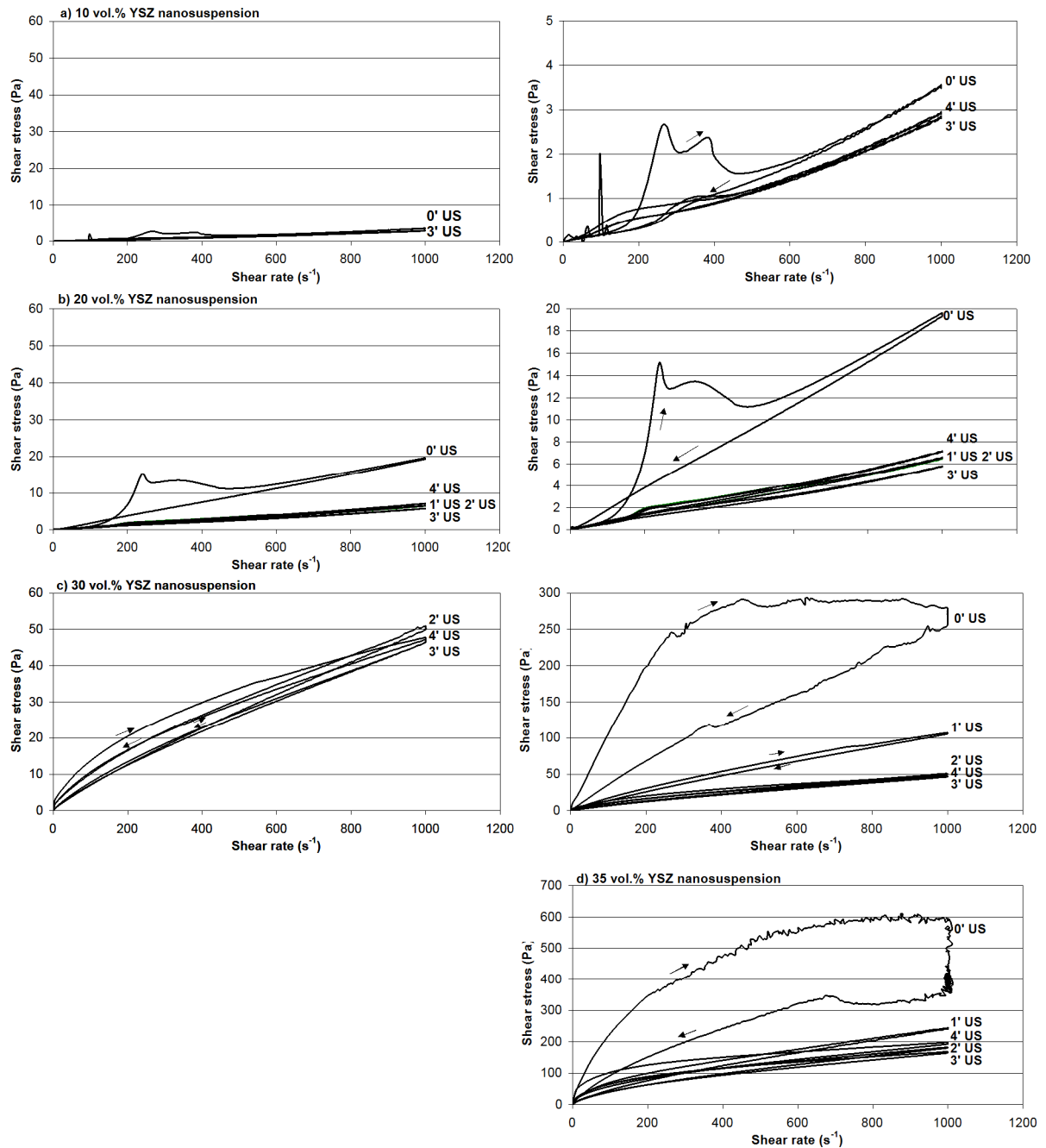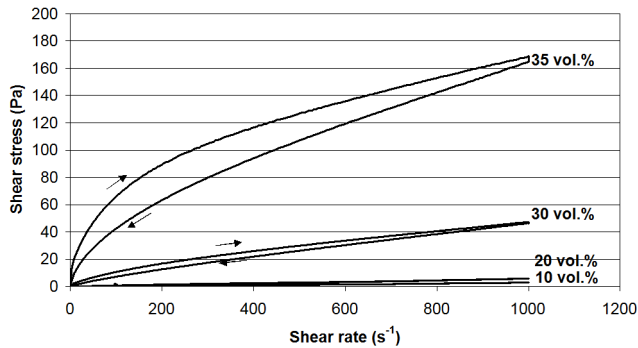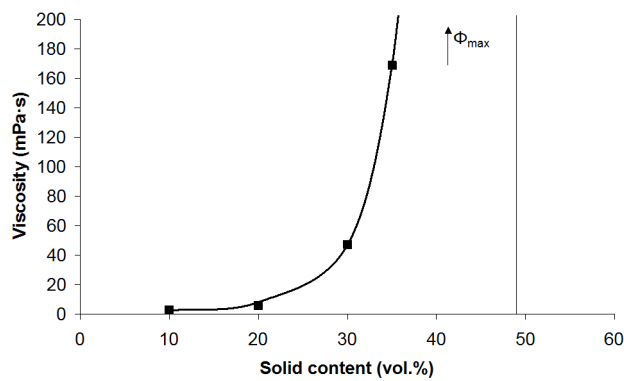
Figure 5

Figure 6 shows rheological behaviour of nanoparticle suspensions with different solid loadings, with optimal sonication time and dispersant content (3 min and 4 PAA%). As expected an increase of the solids content results in higher viscosity and thixotropy. In fact, 35 vol.% suspension was very viscous and thixotropic to be spray-dried. Figure 7 displays the effect of solid loadings in the viscosity. The viscosity values were all taken from the downloading flow curves at a shear rate of 1000 s^{-1} with the optimal sonication time. As it can be seen experimental data fit well to Krieger-Dougherty equation with a correlation coefficient of 0.9997 [31]. Maximum volume fraction (Φ_m) determined by the model was 0.49$\pm$0.04, which is far from the theoretical values for spherical particles

(0.64). However, similar values have been reported in other works with nanoparticle suspensions [12]. Intrinsic viscosity ($[\mu]$) was 8.53 ± 0.15, quite higher than the value of 2.5 theoretically predicted for hard spherical particles suggesting the agglomeration of nanoparticles into irregular shaped agglomerates [12].
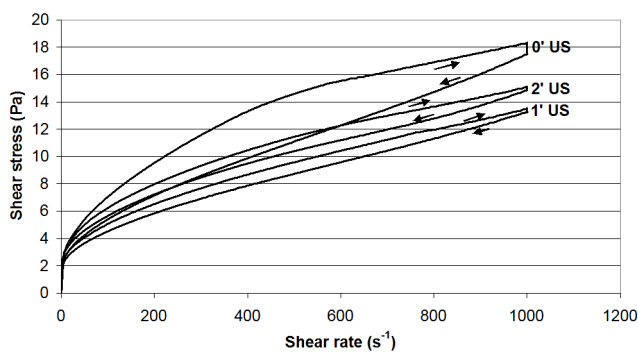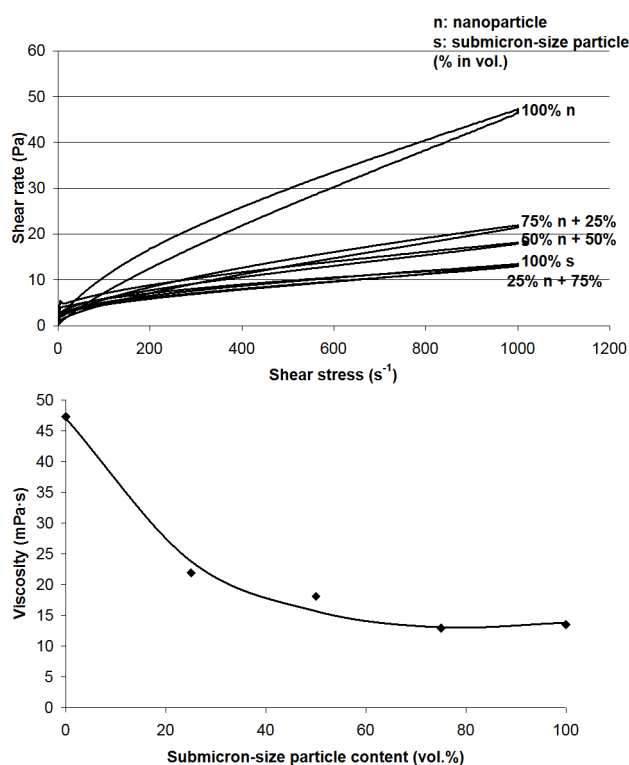

Figure 6

Figure 7

Figure 8 displays the rheological behaviour of 30 vol.% submicron-sized particle suspension prepared with 0.5 % PAA at different sonication times. As observed the optimal time was one minute. If figure 5c and figure 8 are compared, the nanoparticle suspensions at the same solid loading displays higher viscosity.

Figure 8

Figure 9 shows the rheological behaviour of bimodal suspensions with different fine (nanosized)/coarse (submicron-sized) particle ratio. Adding a small amount of submicron-sized particles to a nanoparticle suspension significantly reduces viscosity. Moreover a minimum viscosity starts to occur at a solid loading about 35-40 vol.% of

coarse particles. This finding agrees with particle packing theory for binary mixtures as well as with other nano/submicron-sized particles mixturesreported in previous research [14,23].
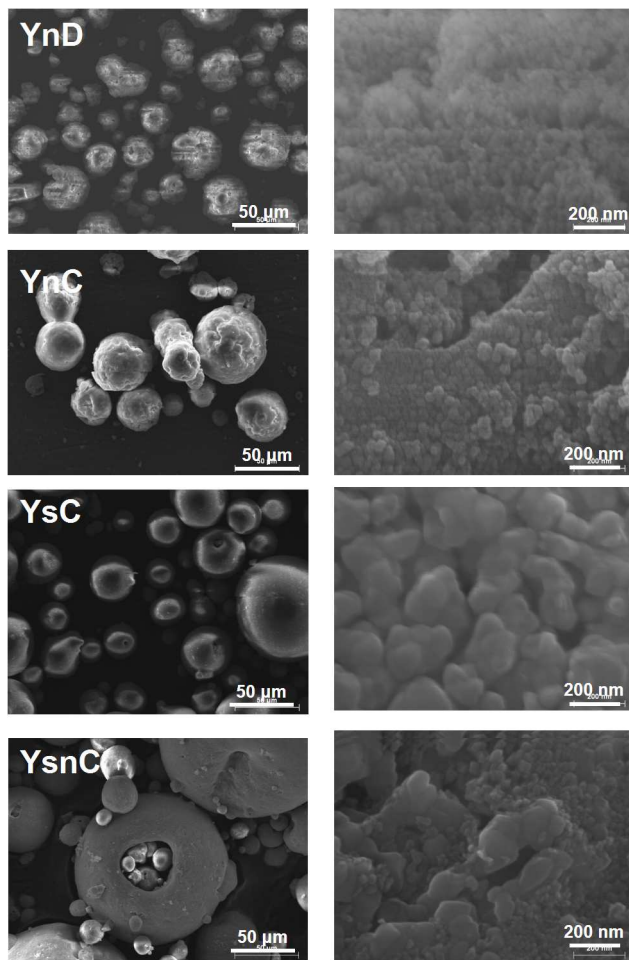

Figure 9

Finally the ageing effect of some prepared suspension was addressed. Hence the rheological behaviour of 30 vol.% suspensions was evaluated 7 days after suspension preparation. Table 3 shows the viscosity measured at shear rate of 1000 s^{-1} and thixotropy of these suspensions. As it can be observed all the suspension aged (increased viscosity) with time. However, suspension obtained from submicron-sized particles hardly shows this effect. Furthermore in binary suspensions an increase of nanoparticle content gives rise to an augmentation of aging. In this sense, although the 100% nanoparticle suspension follows this tendency, the aging effect is less pronounced as a consequence of the high value of viscosity (and thixotropy) of the as-prepared suspension. In fact, this 100% nanoparticle suspension become unstable after hours, or even minutes.

3.3. Spray-drying and thermal treatment processes

Four suspensions with different solid contents and nano/submicron-sized ratios were spray dried. They are summarised in table 4. Figure 10 shows images of the different spray-dry powders at two magnifications. As observed, granules were spherical and some of them displayed the typical doughnut-shape morphology of spray-dried agglomerates [8,9,23]. Furthermore, as expected the corresponding nanosized and submicronsized particles can be distinguished inside the agglomerates.
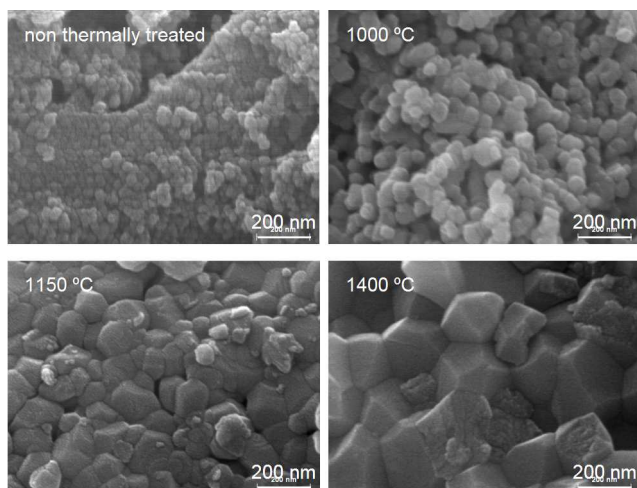
Figure 10

Thermal treatment of the spray-dried powders commonly represents the second step of the reconstitution process for feedstock preparation in APS. In order to establish the beginning of the sintering process and then to determine the heat treatment temperature, tests were conducted in a heating microscope. These tests were carried out on powder samples without any preliminary shaping or compaction of the powder and, thus, the results are actually representative of the feed powder behaviour and not of the sintering process of a given shaped sample or coupon. The evolution of powder contraction as a function of temperature is then plotted. Figure 11 shows the shrinkage versus temperature curves for the four powders detailed in table 4. Unfortunately the test could not achieve the maximum shrinkage value of the different powders since the equipment could not heat over 1400 ºC. Nevertheless, the temperatures to be used for the reconstitution process are more related to the beginning of the sintering process. As observed in this figure samples made up of nanoparticles (YnD and YnC) display much higher sintering rate evaluated from the slope of the contraction-temperature curve profile. On contrary the sintering rate of the submicron-sized powder (YsC) is more gradual whereas the nano/submicron-sized sample (YsnC) displays an intermediate behaviour as a consequence of the presence of submicrometric particles in the powder [16].
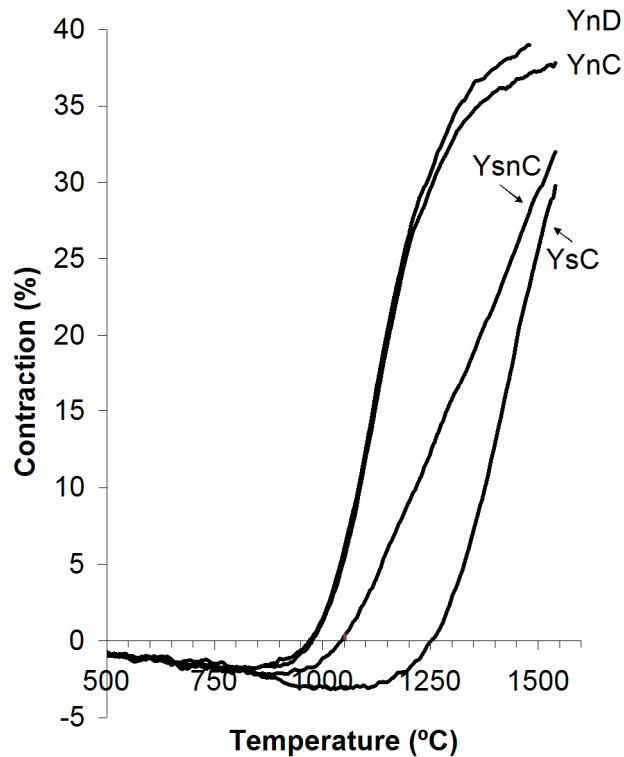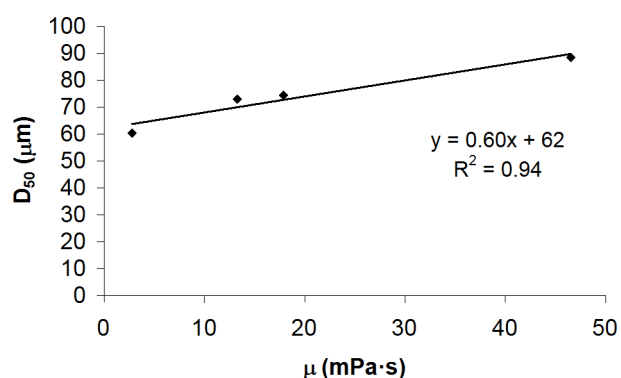
Figure 11

Figure 12 shows the FEG-SEM micrographs of thermally-treated YnC sample at different temperatures. Similar micrographs for a nanostructured, spray-dried powder were previously reported [11,23]. The evolution of the agglomerate microstructure is typical of a solid-state sintering process. This sintering process yields significant changes in sizes and shapes of grains and pores. Grain growth for nanosized particles of the starting agglomerates is apparent at 1150 ℃. Over this temperature the nanostructured nature of the starting powder progressively vanishes. For the submicronsized powder this temperature was about 1235 ℃. Hence the spray dried powders were thermally treated at temperatures in which the shrinkage degree was only incipent (contraction value of around 1%). The same criterion was chosen in previous research [11,23]. Table 4 details the values of these temperatures. These temperatures allow a certain reduction of agglomerates porosity while the nanostructured (or submicrostructured) nature of these agglomerates is mostly preserved.

Figure 12

Thermally treated and non-treated powders were characterised (table 5). Hausner ratio of all reconstituted powders was lower than 1.25 (flowability threshold) which means good flowability [28]. In addition, granule apparent specific mass was sufficiently high (higher than 1700 kg·m^{-3}). All these characteristics make these powders be suitable for APS process [5,23,32].

Furthermore it is worthwhile pointing out the differences between the powders. For thermally untreated samples, on the one hand, granules of nanosized YSZ obtained from concentrated suspensions were denser as a consequence of less water to be evaporated during the spray-drying operation. Likewise, for the same solids content, granules formed by submicron-sized particles were denser than those made up of nanoparticles due to the higher packing efficiency of coarser particles. On the other hand, granule size increased when the viscosity of the starting suspension augmented owing to larger droplet size formed in the spray drying chamber [32,33]. Figure 13 displays the good linear correlation between granule size and suspension viscosity measured at shear rate of 1000 s^{-1}.

Figure 13

As mentioned above during thermal treatment granules densified because of sintering effect. Nevertheless, since the temperature effect of thermal treatment was controlled to preserve the nanostructured nature of the agglomerates the effect of the thermal treatment on granule apparent specific mass was lower than that of the solids content or particle size ratio in the starting suspension. This is a quite important finding because

the characteristics of the APS feedstocks (i.e flowability and agglomerate density) can be governed by the suspension composition and preparation without necessarily detracting the nanostructured or submicronstructured nature of the agglomerates. Besides the agglomerate size hardly change after the thermal treatment.

Finally figure 14 shows XRD patterns of the thermally treated powders. In all cases, the tetragonal was the dominant crystalline phase although a little amount of monoclinic phase was found in the powders containing YSZ nanoparticles due to the presence of this last phase in the starting nanopowder as mentioned above. Nevertheless it should not be a problem since according to literature monoclincal phase in 3YSZ feedstocks transforms into tetragonal phase upon rapid solidification after particle impact and spreading [34].
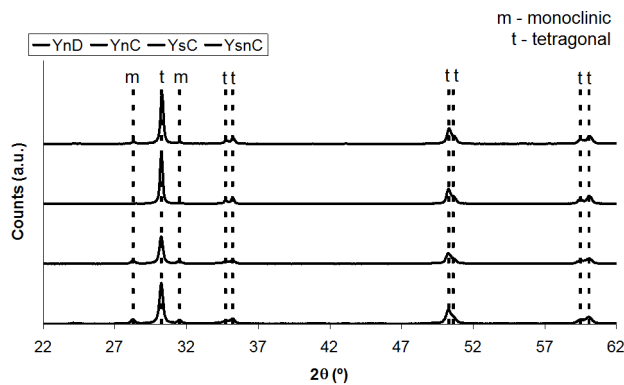
Figure 14

3.4. APS coatings

Thermally treated, reconstituted powders were deposited to obtain APS coatings. Figure 15 sets out the cross-section microstructures of the different coatings at two magnifications.
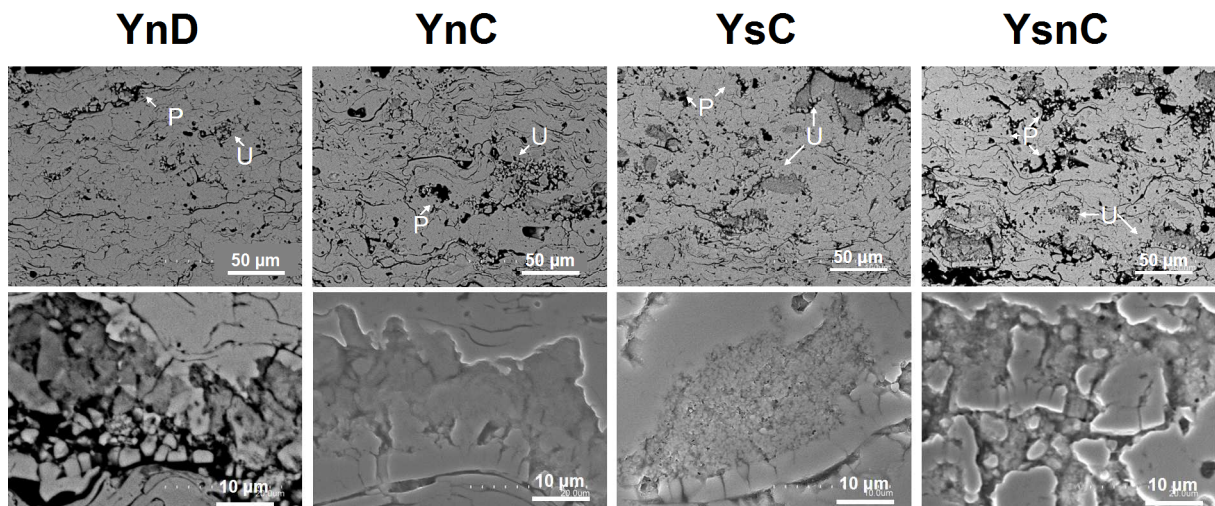
Figure 15

As it can be seen all the coatings were porous, exhibiting the typical lamellar structure of plasma sprayed coatings. Thus smaller pores are located within individual lamellae

and larger pores are found along the interlamellar boundaries The coatings microstructure is clearly influenced by the feedstock characteristics, as revealed by SEM observations The layers deposited from the nanostructured powder (YnD and YnC) exhibit a bimodal microstructure formed by unmelted agglomerates that retained the initial nanostructure, surrounded by a fully melted matrix. Such microstructure has been extensively reported in literature [8,9]. Thus despite the nanostructured character of the primary particles comprising the feedstock, the high porosity associated to these agglomerates results in coatings containing partially melted areas which preserve in some extent the starting nanostructure. Regarding coatings obtained from submicronsized particles (YsC) higher amount of unmelted areas are observed which are made of coarser particles than those comprising the unmelted areas of YnD or YnC coating. An intermediate situation is again observed for the feedstock made up of nano/submicron-sized particles (YnsC). These findings seem to reveal that, for the considered spray operating parameters, feedstock containing more porous granules (like YnD sample) results in coatings less porous and containing fewer amount of unmelted areas because these granules are less resistant to be deformed during the deposition impact [8].

In view of the above, the total porosity of the coatings, as well as the amount of unmelted areas, were estimated by image analysis (Image pro-Plus Bethesada MD, USA) at 500 magnifications, with a resolution around 0.2 µm/pixel, from 10 SEM back-scattering pictures following a procedure set out elsewhere [11,23]. Table 6 shows the porosity and unmelted areas values obtained for all the coatings. It is important to note that small pores, especially nanoporosity inside unmelted zones, cannot be detected by image analysis. Porosity data agree with the typical values observed in these types of coatings. Besides, in all the coatings the porosity values were very similar. This is because, at this low range of coating porosities the contribution of the agglomerate density to the final coating porosity is negligible as compared with the contribution coming from the melting and subsequent deformation of the agglomerates during the deposition process. On contrary larger differences between the coatings were observed for the values of the unmelted areas content. Coatings obtained from feedstocks containing submicronsized particles (YsC and YnsC) display higher amount of unmelted areas in comparison with the feedstocks exclusively formed by nanoparticles (YnD and YnC) in spite of the fact that porosity of YsC and YnsC granules is lower, and consequently their thermal conductivity is higher [5]. Thus for a given plasma spray conditions (plasma energy) the amount and the size of the particles inside these unmelted zones obviously depends on the size of the particles comprising the feedstock agglomerates (nanoparticles or submicron sized particles) but also on other feedstock characteristics such as agglomerate size and density. These findings seem to indicate that denser granules are less prone to splat deformation during deposition provided that all the agglomerates could reach similar melting degree. The highest sinterability of the nanoparticles also influence on the less amount of unmelted zones in YnD and YnC coatings [8].

As observed, the nature and the amount of the unmelted areas in the coatings strongly depend on the characteristics of the feedstock, when considering identical spray operating parameters. Taking into account that the presence of these nanozones can positively affect some thermal and mechanical properties in the final coatings [8,9] it is still necessary further research so as to relate the microstructures set out in this research with the properties of the coatings obtained.

4. Conclusions

In this study, YSZ aqueous suspensions prepared from submicron- and nano-sized particles with different solid loadings were stabilised by means of Z-potential measurements. The effect of sonication time, dispersant content and ageing was evaluated. Viscosity at different solid loading fitted to Krieger-Dougherty equation. A minimum of viscosity was found when around 35 vol.% submicronsized particles were mixed with nanoparticles.

Then YSZ reconstituted powders were obtained from these suspensions. The reconstitution process consisted in spray-drying of the suspension followed by thermal treatment. The optimal temperature for the treatment was found from sintering data and microstructural observation. The resulting powders displayed good flowability and high apparent specific weight so that they can be deposited by atmospheric plasma spraying without any problems. In addition, a linear correlation exists between the suspension viscosity and the granule size.

APS coatings were obtained from the YSZ reconstituted powders. They show bimodal microstructure in which unmelted nanostructured or submicrostructured zones were surrounded by a melted matrix. However, the amount of these unmelted areas was lower in the case of the coating obtained from nanostructured feedstock owing to the higher deformability of the agglomerates comprising this powder during splat deposition.

Reference

[1] Gogotsi GA, Galenko VI, Mudrik SP, Ozerski BI, Khvorostyany VV, Khristevich TA. Fracture behaviour of YSZ ceramics: New outcomes. Ceram Inter 2010;36:345-50.

[2] Pradhan M, Kapur PC. Effect of powder dispersion on sintering behaviour and mechanical properties of nanostructured 3YSZ ceramics. Ceram Inter 2012;38:2835-43.

[3] Hu L, Wang C, Hu Z. Porous yttria-stabilized zirconia ceramics with ultra-low thermal conductivity. Part II: temperature dependence of thermophysical properties. J Mater Sci 2011;46:623-28.

[4] Vassen R, Stuke A, Stöver D. Recent developments in the field of thermal barrier coatings. Therm Spray Technol 2009;18:181-86.

[5] Fauchais P, Montavon G, Bertrand G. From powders to thermally sprayed coatings. Therm Spray Technol 2009;19:56-80.

[6] Chawla V, Sidhu BS, Puri D, Prakash S. Performance of plasma sprayed nanostructured and conventional coatings. J Aus Ceram Soc 2008;44:56-62.

[7] Gel M, Jordan EH, Sohn YH, Goberman D, Shaw L, Xiao TD. Development and implementation of plasma sprayed nanostructured ceramic coatings, Surf Coat Technol 2001;146-47:48-54.

[8] Lima RS, Marple BR. Thermal spray coatings engineered from nanostructured ceramic agglomerated powders for structural, thermal barrier and biomedical applications: A review. J Therm Spray Technol 2007;16:40-63.

[9] Pawlowski L. Finely grained nanometric and submicrometric coatings by thermal spraying: A review. Surf Coat Technol 2008;205:4318-28.

[10] Yang Y, Wang, Y, Wang Z, Liu G, Tian W. Preparation and sintering behaviour of nanostructured alumina/titania composite powders modified with nano-dopants. Mat Sci Eng A 2008;490:457-64.

[11] Sánchez E, Moreno A, Vicent M, Salvador MD, Bonache V, Klyatskina E, Santacruz I, Moreno R. Preparation and spray drying of Al_2O_3-TiO_2 nanoparticle suspensions to obtain nanostructured coatings by APS. Surf Coat Technol 2010;205:987-92.

[12] Vicent M, Sánchez E, Moreno A, Moreno R. Preparation of high solids content nano-titania suspensions to obtain spray-dried nanostructured powders for atmospheric plasma spraying. J Eur Ceram Soc 2012;32:185-94.

[13] Fazio S, Guzmán J, Colomer MT, Salomoni A, Moreno R. Colloidal stability of nanosized titania aqueous suspensions. J Eur Ceram Soc 2008;28:2171-76.

[14] Santacruz I, Anapoorani K, Binner J. Preparation of high solids content nanozirconia suspensions. J Am Ceram Soc 2008;91:398-405.

[15] Fengqiu T, Xiaoxian H, Yuferg Z, Jingkun G. Effect of dispersants on surface chemical properties of nano-zirconia suspensions. Ceram Int 2000;26:93-7.

[16] Benavente R, Salvador MD, Alcázar MC, Moreno R. Dense nanostructured zirconia compacts obtained by colloidal filtration of binary mixtures. Ceram Int 2010;38:2111-7.

[17] Calambás HL, Liliana BG, Albano MP. Processing of different alumina-zirconia composites by slip casting. Ceram Int 2013;39:6657-67.

[18] Ramanathan S, Krishnakumar KP, Banerjee PKS. Powder dispersion and aqueous tape casting of YSZ_NiO composite. J Mater Sci 2004;39:3339-44.

[19] Raghupathy BPC, Binner JGP. Spray granulation of nanometric zirconia particles, J Am Ceram Soc 2011;94:139-45.

[20] García E, Mesquita-Gimarâes J, Miranzo P, Osendi MI. Porous mullite and mullite-ZrO_2 granules for thermal spraying applications. Surf Coat Technol 2011;205:4304-11.

[21] Loghman-Estarki MR, Edris H, Razavi RS, Ghasemi R, Pourbafrany M, Ramezani M. Spray drying of nanometric SYSZ powders to obtain plasma sprayable nanostructured granules. Ceram Int 2013;39:9447-9457.

[22] Qin K, Zaman AA. Viscosity of concentrated colloidal suspensions: comparison of bidisperse models. J Colloid Interface Sci 2003;266:461-7.

[23] Vicent M, Bannier E, Moreno R, Salvador MD, Sánchez E. Atmospheric plasma spraying coatings from alumina-titania feedstock comprising bimodal particle size distributions. J Eur Ceram Soc 2013;33:3313-24.

[24] Candelario VM, Guiberteau F, Moreno R, Ortiz AL. Aqueous colloidal processing of submicrometric SiC plus $Y_3Al_{15}O_{12}$ with diamond nanoparticles. J Eur Ceram Soc 2013;33:2473:2482.

[25] Burgos-Montes O, Moreno R. Stability of concentrated suspensions of Al_2O_3-SiO_2 measured by multiple light scattering. J Eur Ceram Soc 2009;29:603-10.

[26] Gutiérrez CA, Moreno R. Preventing ageing on Al_2O_3 casting slips dispersed with polyelectrolytes. J Mater Sci 2000;35:5867-72.

[27] Vicent M, Sánchez, E, Santacruz, I, Moreno R. Dispersion of TiO_2 nanoparticles to obtain homogeneous nanostructured granules by spray-drying. J Eur Ceram Soc 2011;31:1413-19.

[28] Amorós JL, Blasco A, Enrique JE, Negre F. Características de polvos cerámicos para prensado [Characteisitics of ceramic powders for pressing]. Bol Soc Esp Ceram Vidr 1987;79:3033-40.

[29] Wu L, Huang Y, Wang Z, Liu L. Interaction and dispersion stability of alumina suspension with PAA in N,N'-dimethylformamide. J Eur Ceram Soc 2010;30:1327-33.

[30] Garmendia N, Santacruz I, Moreno R, Obieta I. Slip casting of nanozirconia/MWCNT composites using a heterocoagulation process. J Eur Ceram Soc 2009;29:1939-45.

[31] Krieger IM, Dougherty TJ. A mechanism for non-Newtonian flow in suspensions of rigid spheres. Trans Soc Rheol 1959;3:137–52.

[32] Cao XQ, Vassen R, Schwartz S, Jungen W, Tietz F, Stöever D. Spray-drying of ceramics for plasma-spray coating. J Eur Ceram Soc 2000;20:2433-9.

[33] Walker WJ, Reed JS. Influence of slurry parameters on the characteristics of spray-dried granules. J Am Ceram Soc 1999;82:1711-9.

[34] Carpio P, Rayón E, Pawlowski L, Cattini A, Benavente R, Bannier E, Salvador MD, Sánchez E. Microstructure and indentation mechanical properties of YSZ nanostructured coatings by suspension plasma spraying. Surf Coat Technol 2013;220:237-43.

[35] Marple BR, Lima RS. Engineering nanostructured thermal spray coatings: process-property-performance relationships of ceramic based materials. Adv Appl Ceram 2007;106:265-75.

Tables

Table 1. Main characteristics of the raw materials provided by the suppliers

	Nanoparticles	Submicron-sized powder
$Y_2O_3 : ZrO_2$ mol ratio	3:97	3:97
Density (kg/m^3)	5900	6050
Main phase	Tetragonal	Tetragonal
Average particle size (nm)	40	400

Table 2. Main plasma spraying parameters

	Bond coat	YSZ
Ar flow rate (slpm*)	68	35
H$_2$ flow rate (slpm*)	8	12
Intensity (A)	650	600
Anode nozzle internal diameter (mm)	6	6
Spraying distance (mm)	145	100
Spraying speed (m/s)	1	1
Scanning step (mm)	2	4
Sample cooling	front and behind	front and behind
Feedstock injector diameter (mm)	1.5	2.0
Feedstock mass flow rate (g/min)	40	45

$*$slpm: standard litre per minute

Table 3. Viscosity and thixotropy of aged and non-aged suspensions

		Viscosity (mPa·s)	Thixotropy (Pa/s)
100% nano	0 days	46.5	3030
	7 days	61.9	2000
75% nano + 25% submicron	0 days	21.5	1510
	7 days	60.2	2820
50% nano + 50% submicron	0 days	17.9	880
	7 days	26.2	116
25% nano + 75% submicron	0 days	12.9	800
	7 days	18.4	580
100% submicron	0 days	13.3	540
	7 days	14.6	270

Table 4. List of the different spray-dried powders and the selected temperature of each one for the thermal treatment

Reference	Raw materials	Solid loading	T (ºC)
YnD	Nano-sized YSZ	10 vol.%	1000
YnC	Nano-sized YSZ	30 vol.%	1000
YsC	Submicron-sized YSZ	30 vol.%	1200
YsnC	50 wt% nano- + 50 wt% submicron-sized YSZ	30 vol.%	1050

Table 5. Characteristics of the reconstituted powders

Reference	Hausner ratio	$\rho_{granule}$ (kg/m^3)	$D_{v,50}$ (µm)
YnD untreated	1.18±0.03	2050±40	57±8
YnD thermally treated	1.24±0.03	2230±30	60±6
YnC untreated	1.11±0.03	2570±30	94±9
YnC thermally treated	1.20±0.03	2750±30	88±9
YsC untreated	1.15±0.03	3300±30	63±6
YsC thermally treated	1.22±0.03	3710±30	72±7
YsnC untreated	1.13±0.03	3020±30	74±7
YsnC thermally treated	1.20±0.03	3200±40	74±7

Table 6. Porosity and unmelted area values (%) in the coatings

Coating	Porosity (%)	Unmelted areas (%)
YnD	7.1±1.0	1.2±0.2
YnC	7.9±1.3	2.5±0.7
YsC	8.2±1.0	8.0±1.0
YsnC	7.2±1.3	7.5±0.9